Review

Infrared spectroscopy: A potential tool in huanglongbing and citrus variegated chlorosis diagnosis

Marcelo Camponez do Brasil Cardinali [a,b], Paulino Ribeiro Villas Boas [a,*],
Débora Marcondes Bastos Pereira Milori [a], Ednaldo José Ferreira [a], Marina França e Silva [a,b],
Marcos Antonio Machado [c], Barbara Sayuri Bellete [d], Maria Fatima das Graças Fernandes da Silva [d]

[a] Embrapa Instrumentação, Rua XV de Novembro 1452, CEP 13560-970 São Carlos, SP, Brazil
[b] Instituto de Física de São Carlos, Universidade de São Paulo, Av. Trabalhador São-Carlense 400, CEP 13566-590 São Carlos, SP, Brazil
[c] Centro de Citricultura Sylvio Moreira, IAC, Rodovia Anhanguera, km 158, CEP 13490-970 Cordeirópolis, SP, Brazil
[d] Departamento de Química, Universidade Federal de São Carlos, Rodovia Washington Luís, km 235, SP-310, CEP 13565-905 São Carlos, SP, Brazil

ARTICLE INFO

ABSTRACT

Huanglongbing (HLB) and citrus variegated chlorosis (CVC) are serious threats to citrus production and have caused considerable economic losses worldwide, especially in Brazil, which is one of the biggest citrus producers in the world. Neither disease has a cure nor an efficient means of control. They are also generally confused with each other in the field since they share similar initial symptoms, e.g., yellowing blotchy leaves. The most efficient tool for detecting these diseases is by polymerase chain reaction (PCR). However, PCR is expensive, is not high throughput, and is subject to cross reaction and contamination. In this report, a diagnostic method is proposed for detecting HLB and CVC diseases in leaves of sweet orange trees using attenuated total reflectance Fourier transform infrared spectroscopy and the induced classifier via partial least-squares regression. Four different leaf types were considered: healthy, CVC-symptomatic, HLB-symptomatic, and HLB-asymptomatic. The results show a success rate of 93.8% in correctly identifying these different leaf types. In order to understand which compounds are responsible for the spectral differences between the leaf types, samples of carbohydrates starch, sucrose, and glucose, flavonoids hesperidin and naringin, and coumarin umbelliferone were also analyzed. The concentration of these compounds in leaves may vary due to biotic stresses.

© 2012 Published by Elsevier B.V.

Contents

1. Introduction

Citrus production is one of the most important economic agricultural activities in the world. Annually, approximately 122 millions of tons of citrus fruits, including oranges, grapefruits,

* Corresponding author. Tel.: +55 16 2107 2800; fax: +55 16 2107 2902.
  E-mail address: paulino@cnpdia.embrapa.br (P.R. Villas Boas).

lemons, and tangerines, are produced, corresponding to roughly US$ 17 billion from the sale of juices and fresh fruit worldwide in 2008, according to the Food and Agriculture Organization of the United Nations [1]. However, economic losses in citrus production have occurred in recent years due to diseases such as huanglongbing (HLB) and citrus variegated chlorosis (CVC). HLB is a serious threat to world production, as it has rapidly spread through the orchards of many countries, especially the world's largest citrus producers, Brazil and the United States. CVC is a disease commonly found in orchards in Brazil and has also caused several losses in recent years.

CVC is caused by *Xylella fastidiosa*, which colonizes the xylem vessels and disrupts the transport of water and nutrients from the root system to the canopy [2]. It affects all sweet orange varieties equally and can be transmitted by leafhoppers, contaminated budwood, and seedlings [3]. Field management of CVC involves the planting of healthy seedlings, chemical control of the vectors, pruning of infected branches in trees more than 6 years old, and eradication of diseased trees younger than 5 years old [3]. The estimated control cost in São Paulo State, Brazil, is nearly US$ 100 million [3]. Symptoms in sweet orange include bright yellow leaf mottle with distinct lesions on the adaxial leaf surface [2]. In older leaves, these lesions extend through the leaf to form gummy blisters similar to lesions on the abaxial leaf surface. On severely affected trees, the internodes are markedly shortened, and the leaves are abnormally small. Fruits remain small and hard at harvest time [4].

HLB is caused by a phloem-limited bacterium provisionally named *Candidatus* Liberibacter spp., and its vector is the citrus psyllid *Diaphorina citri* [5]. No sources of resistance are known within the citrus group, and the pathosystem is poorly understood. All varieties of sweet oranges and mandarins are highly susceptible to HLB. HLB has been controlled by planting certified healthy seedlings, eradicating symptomatic trees found in the orchard, and chemically spraying for the vector. Typical HLB symptoms include blotchy asymmetric yellowing leaves and deformed fruits [6]. In some cases the leaves may become thicker with enlarged veins [6]. The fruits are generally bitter, small, and deformed, with a thicker albedo and aborted seeds. Some fruits may also display blotchy mottle symptoms [7]. The asymptomatic phase can last from 6 months to 2 years [8], making the infected tree an undetectable source of the disease in the field.

Several studies have attempted to elucidate the chemical changes caused by HLB and CVC. Several reports have shown the accumulation of starch in the leaves of trees infected with HLB [9–12]. Fan et al. [9] also found changes in different carbohydrate concentrations in healthy, HLB-symptomatic, and HLB-asymptomatic leaves. While starch and sucrose increase in HLB-asymptomatic and HLB-symptomatic leaves when compared to healthy ones, maltose progressively decreases from healthy to symptomatic leaves. A significant increase has also been observed in the fructose concentration of asymptomatic leaves when compared to healthy or symptomatic counterparts.

The concentration of secondary metabolites may also differ in diseased trees, as shown in other studies [13–16]. It has been reported that the concentration of the flavonoid hesperidin increases in the leaf mesophyll cells of trees affected by CVC [13]. Other secondary metabolites also suggest CVC infection, such as phytoalexins, which are antimicrobial substances that accumulate after infection by pathogens [14]. The accumulation of antifungal compounds, such as coumarins, in citrus tissues has been observed after inoculation with *Phytophthora citrophthora* [15]. Afek et al. [16] showed that the concentration of umbelliferone (7-hydroxycoumarin) increased considerably in the albedo of immature grapefruits compared to the albedo of mature fruits after inoculation with *Penicillium digitatum*.

The diagnosis of HLB and CVC is generally performed by the quantitative real-time polymerase chain reaction (PCR) [17–20], which detects the bacterium with high accuracy by using its genetic code. This method, however, is expensive and laborious, and hence, it is ill-suited for large-scale use. Furthermore, since the HLB and CVC bacteria distributions inside the whole tree are not uniform [17,20], the diseases may not be diagnosed by this method in the analyzed samples if the corresponding bacteria are absent.

Spectroscopic methods appear to be promising alternatives for the diagnosis of citrus diseases since they can rapidly measure the optical properties of the samples that are related to their chemical composition. Such methods have already been employed for investigating chemical changes in HLB disease trees [12,21–26]. Based on the concentrations of several elements, Pereira et al. [21] identified differences not only in healthy and HLB-symptomatic leaves, but also in HLB-asymptomatic and healthy leaves with a 90% success rate. Pereira et al. [22] also showed that infected young trees with HLB can be diagnosed some months after inoculation even in the asymptomatic phase using laser-induced breakdown spectroscopy (LIBS). In these studies, no other diseases were considered.

Using mid-infrared spectroscopy, Sankaran et al. [12] distinguished HLB-symptomatic leaves from healthy and nutrient-deficient leaves with a 90% success rate. Hawkins et al. [25] employed attenuated total reflectance Fourier transform infrared (ATR-FTIR) spectroscopy to compare several diseases, such as tristeza, citrus leaf rugose, citrus psorosis, and citrus canker, and deficiencies of nutrients, including iron, copper, zinc, manganese, and magnesium, with HLB-symptomatic and healthy trees. They reported that leaves from trees with certain nutrient deficiencies and with citrus canker could not be distinguished from HLB-positive trees. In another analysis, Hawkins et al. [26] compared healthy trees with HLB-infected trees at several stages, including asymptomatic trees, using ATR-FTIR. They achieved a 95% success rate, however, few asymptomatic trees were considered.

Although infrared spectroscopy has been applied to distinguish healthy trees or leaves from nutrient-deficient, HLB-symptomatic, and HLB-asymptomatic trees or leaves, all samples in the previous analyses [12,25,26] were derived from temperate zones and required preparation (e.g., grinding). The leaves considered in this article were collected from trees in tropical zones and were measured *in natura*. Also, in previous analyses, HLB-infected leaves were compared to neither CVC-infected leaves nor secondary metabolites.

In this article, ATR-FTIR spectroscopy is employed to identify differences between healthy, HLB-symptomatic, HLB-asymptomatic, and CVC-symptomatic leaves. Samples of carbohydrate starch, sucrose, and glucose, flavonoids naringin and hesperidin and the coumarin umbelliferone were examined to determine whether these compounds show the spectral characteristics that may contribute to the spectral differences observed between the leaves analyzed.

2. Materials and methods

2.1. Samples

Leaves were collected from healthy, HLB-, and CVC-infected adult trees of Valencia sweet orange (*Citrus sinensis* L. Osbeck) grafted onto Swingle citrumelo (*Citrus paradisi* Macf. × *Poncirus trifoliata* L. Raf.), located at the Fisher Group's farm in the city of Mat ao (State of São Paulo, Brazil). All infected trees considered had typical HLB or CVC symptoms and were identified by qualified inspectors. Healthy trees were chosen from grove blocks without HLB or CVC infestation and were free of any other type of stress. All plants were grown under the same soil, water, nutrient, and pesticide conditions.
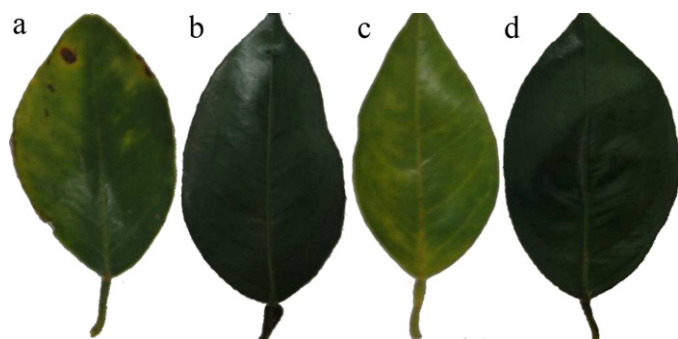
Fig. 1. Examples of CVC (a), healthy (b), HLB-symptomatic (c), and HLB-asymptomatic (d) leaves, illustrating their differences. HLB- and CVC-symptomatic leaves are commonly confused because they have similar color patterns, although the former can sometimes have black stains as in (a). The difficulty in separating these four classes lies in distinguishing healthy (b) from HLB-asymptomatic (d) leaves due to the lack of visual differences.

Eight trees of each condition (healthy, HLB, and CVC) were considered. Healthy leaves were randomly collected from the external part of the tree canopy at around 1.5 m from the ground. All CVC- and HLB-symptomatic leaves had typical visible symptoms. HLB-asymptomatic leaves were collected from trees with typical symptoms of HLB in the same way as healthy leaves but by avoiding branches that had symptomatic leaves. The conditions of the leaves, i.e., healthy, CVC, HLB-symptomatic, and HLB-asymptomatic, are henceforth called classes. A total of 40 leaves of each class were collected. Fig. 1 shows an example of each class of leaves collected. After being collected, the leaves were transported the same day. In the laboratory, the leaves were cleaned with cotton moistened with distilled water and kept in plastic bags refrigerated at temperatures of about 5 °C. Measurements were taken within 3 days of collection.

Potassium bromide (KBr) pellets were prepared with starch, sucrose, and glucose standard samples, and with hesperidin, naringin, and umbelliferone commercial samples. Each pellet was obtained by crushing 1 mg of each compound with 100 mg of KBr dried powder and pressing it into a die with a pressure of 5 tons for 5 min.

2.2. FTIR measurements

A Perkin Elmer Spectrum 1000 with a detector based on $LiTaO_3$ (lithium tantalate) crystal was used for FTIR measurements, along with Spectrum version 5.3 acquisition software. All measurements were made with leaves *in natura* on the adaxial side, next to the midrib. The leaves were placed on the ATR crystal, which was made of zinc selenide, to collect the surface spectra. The KBr pellets were placed in a pellet holder. For each sample, 32 scans were made at a range of 4000–700 cm^{-1}, with spectral resolution of 4 cm^{-1}. For all measures, the equipment room was maintained at 21 °C and 30–35% relative air humidity. To eliminate the influence of the equipment and the atmospheric conditions on the measurements, a background spectrum was collected before collecting the spectra of the leaves. For the carbohydrates and metabolites, a pure KBr pellet was measured for background. After each measure, the ATR crystal was cleaned with acetone and cotton. Leaves of different classes were measured in random order to eliminate any chance of biased results.

2.3. Dataset treatment and classification model

The leaf spectral dataset was preprocessed using the Spectrum version 5.1 equipment software from Perkin Elmer, which corrected the spectrum baselines by using a quadratic function. Then,

the spectral offsets were adjusted by setting the minimum absorption to zero, and spectra were normalized by their respective areas. The normalization step was performed to emphasize the local differences between the peaks and the bands (spectral profile) and to reduce the influence of the intensity of the whole spectra. The water absorbance region was ignored, selecting a range of 1530–700 cm^{-1} to induce the classifier.

Classification was performed by an induced classifier via partial least square regression (PLSR). PLSR is a method widely used in chemometrics [27] for evaluating the concentration of chemical compounds in samples from their emission, absorption, reflectance, transmittance, or fluorescence spectra. This method is characterized by finding a linear transformation in the predictor variables (the spectral points) that provides the best correlation with the response variables (the concentration of the chemical compounds). The main advantage of PLSR is to use the linear correlation between the predictor variables to build the regression model.

To apply PLSR to classification problems, the classes must be identified as numbers (see [28]). The induced classifier via regression associates classes with numbers using a process known as binarization, in which a value of 1 is attributed to a reference class and a value of 0 is attributed to the others. Therefore, for each class, one leaf spectral dataset equal to the original one is created and is split into training and test sets. The first set is used to adjust the regression method, while the second validates it. For each element of the test set, the adjusted regression method returns a value between 0 and 1. The higher the value is, the higher the similarity is between the corresponding spectrum and the reference class. The same procedure is then repeated for all classes using the same training and test sets. Thus, one value between 0 and 1 is obtained for each spectrum tested and for each class. The spectrum tested is assigned to the class with the highest value returned by the regression methods. For each spectrum tested, the classifier also provides for each class a prediction probability that is proportional to the corresponding value returned by the regression models. Such a probability may be used as an indicator of the quality of a given assignment performed by the classifier.

The classifier accuracy was evaluated by 10 realizations of 10-fold stratified cross-validation, where the dataset is randomly partitioned into 90% for training and 10% for testing. The process of cross-validation is iterated with different random partitions, and the results are averaged. This procedure is applied to ensure that the accuracy will not be biased due to a particular partitioning of training and test sets. The dataset used in the classifier was mean centered, and the first 20 components were used in the PLSR model.

3. Results and discussion

The results are presented in two subsections. The first subsection describes and explains the spectral differences between the classes, and the second subsection presents and discusses the results obtained by the induced classifier via PLSR.

3.1. Spectral differences

Fig. 2 shows typical spectra of healthy, HLB-asymptomatic, HLB-symptomatic, and CVC leaves, normalized by area. These typical spectra of healthy and diseased leaves were chosen according to the prediction probability obtained by the induced classifier, the results of which will be presented in the next subsection. Thus, the typical spectrum of each leaf type is the one that has the highest prediction probability for the corresponding class, i.e., the typical spectrum is the one that best represents the respective leaf type.
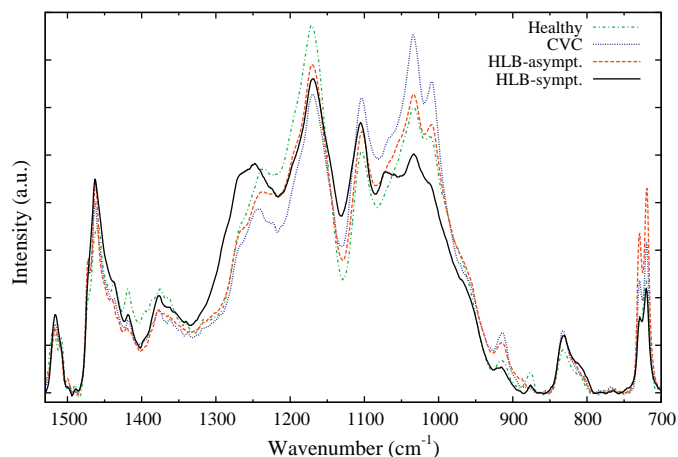
Fig. 2. Typical normalized FTIR spectra of all leaf types.

Fig. 3. Normalized FTIR spectra of KBr pellets of starch, glucose, and sucrose standard samples.

In Fig. 2, many differences between the spectra of leaves can be observed, especially from 1300 to 900 cm^{-1}. The peak at 1437 cm^{-1} is only well defined for the healthy leaf spectrum. The band of the HLB-symptomatic spectrum at 1250 cm^{-1} is broad, deformed, and shifted in comparison to the bands of the other spectra. The ratio between intensities of peaks can also be useful to differentiate the leaf types, e.g., between the peaks at 1170 and 1105 cm^{-1}, at 1170 and 1035 cm^{-1}, at 1419 and 1377 cm^{-1}, at 913 and 877 cm^{-1}, and at 832 and 720 cm^{-1}. In addition, other spectral differences are not clearly visible in Fig. 2 that may also help to distinguish the leaf types. Finding the pattern which best characterizes each leaf type is not an easy task, especially when the differences are not so clear. Such a task is then performed by classifiers which automatically determine the best combination of spectral points that defines each leaf type.

The range of 1175–900 cm^{-1} is generally associated with the absorption of starch [12,25,26], the concentration of which is expected to be different between healthy and HLB (either symptomatic or asymptomatic) leaves [9–12]. However, it is not possible to assign this range only to the absorption of carbohydrates because other chemical substances in the leaves may also absorb infrared light-for instance, secondary metabolites. Moreover, the concentrations of secondary metabolites may be different when comparing a healthy leaf to a diseased leaf and may also contribute to distinguishing them. To understand which chemicals are responsible for the spectral variations observed in Fig. 2, FTIR measurements were performed on samples of carbohydrates and secondary metabolites. Fig. 3 shows the normalized spectra of starch, glucose, and sucrose standard samples. Fig. 4 exhibits the spectra of the flavonoids hesperidin and naringin and the coumarin umbelliferone produced by citrus trees.

The obtained spectra shown in Figs. 3 and 4 are similar to those found in Spectral Database for Organic Compounds from the National Institute of Advanced Science and Technology [29]. Among the flavonoids, hesperidin is one of the most abundant secondary metabolites in the leaves of Valencia sweet orange (about 5 mg/g); the presence of naringin was not verified in healthy leaves of the same variety [30]. Although other abundant flavonoids are present in citrus leaves [30], such as rutin, diosmin, nobiletin, and isorhoifolin, that were not considered in this analysis, the spectra of the secondary metabolites shown in Fig. 4 provide strong evidence that their contributions are crucial to understanding the peaks and bands in the ranges 1530–1175 cm^{-1} and 900–700 cm^{-1} in Fig. 2, where the carbohydrates do not have peaks or bands similar to the leaf spectra (see Fig. 3). In addition, the bands at 1515 and
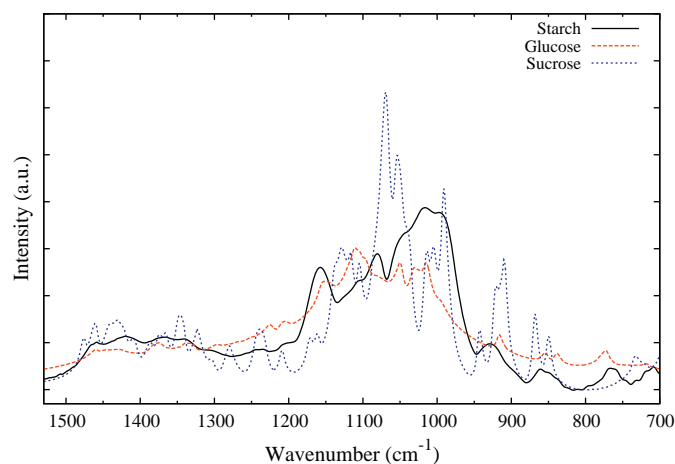
1450 cm^{-1} in Fig. 2 could be associated with the vibrational modes of hesperidin and umbelliferone (see Fig. 4).

3.2. Classifier induced results

Table 1 shows the confusion matrix of the induced classifier via PLSR. The columns of this matrix represent the assigned classes by the classifier, and the rows, the nominal classes. Each value in this table corresponds to the portion of a nominal class that was assigned by the induced classifier to a certain class. The sum of each row is 100%. Each diagonal element is the success rate per class, and the average of the matrix trace represents the total success rate of the classifier, which is 93.8%. The standard deviation of the classification was 6.3%.

According to Table 1, HLB-symptomatic is the class with the highest success rate, followed by CVC and HLB-asymptomatic. The lowest success rate was obtained for the healthy class, with a success rate of 89.25%. Curiously, the misclassification rate between healthy and HLB-asymptomatic leaves, which are visually similar (see Fig. 1), was one of the lowest. The misclassification between the HLB-symptomatic and the HLB-asymptomatic leaves may not be considered an error because they represent the same disease at different stages. Since the misclassification rates between different classes are low (less or equal than 6%), the classes do in fact have different chemical compositions, which were differentiated
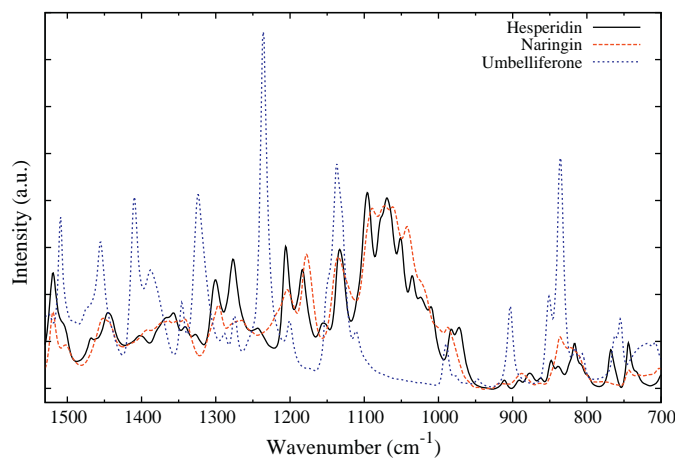

Fig. 4. Normalized FTIR spectra of KBr pellets of flavonoids and coumarin commercial samples.

Table 1
Confusion matrix of the induced classifier via PLSR with 10 realizations of 10-fold stratified cross-validation. The columns correspond to the assigned classes of the classifier, and the rows correspond to the nominal classes. The classifier achieved a success rate of 93.8% (the average of the matrix trace) with a standard deviation of 6.3%.

Nominal class	CVC	Healthy	HLB-asympt.	HLB-sympt.
CVC	95.00%	2.50%[a]	2.50%[a]	0.00%
Healthy	3.25%[a]	89.25%	1.50%[a]	6.00%[a]
HLB-asympt.	3.25%[a]	3.00%[a]	93.75%	0.00%
HLB-sympt.	0.00%	2.50%[a]	0.25%[a]	97.50%

[a] Incorrect predictions.

Table 2
Fraction of incorrect predictions for prediction probabilities greater than a given threshold. Results obtained by induced classifier via PLSR with 10 realizations of 10-fold stratified cross-validation using the Waikato Environment for Knowledge Analysis (WEKA) [31].

Threshold (%)	Fraction of incorrect predictions (%)
30	100.00
40	91.92
50	51.51
60	19.19
70	6.06
80	1.01
90	0.00

by infrared spectroscopy analysis. Such differences were then uncovered by the induced classifier via PLSR.

In addition to the analysis of the confusion matrix, it is also possible to analyze the prediction probability of each leaf tested. This probability indicates the degree of similarity between the leaf tested and the classes obtained by the induced classifier. Thus, the higher the prediction probability, the greater the similarity between the leaf tested and the trained class. For example, if the prediction probability for a leaf tested is 100% for a given class, then this leaf has no similarity with the other classes. With lower values, the chance of having an incorrect prediction increases. Table 2 exhibits the portion of errors for prediction probabilities greater than a given threshold. The proportion of errors quickly decreases as the prediction probability increases. For example, for a prediction probability above 70%, the proportion of errors is only 6.06%. The proportion of errors can then be used as an index of the quality of the predictions of the classifier. Thus, based on that index, the producer can make better decisions.

The robustness of the induced classifier via PSLR may be a result of the spectral differences found between the classes and the efficiency of the PLSR model used to uncover such differences. Although these differences exist and may be related to variations in carbohydrate and secondary metabolites (see Figs. 2–4), further analyses have to be conducted in order to verify which chemical molecules are being altered in the evolution of diseases in citrus trees. Such analyses will help to improve the classifier and the detection rate of CVC and HLB diseases.

4. Conclusions

This study shows that ATR-FTIR spectroscopy can be used to diagnose HLB and CVC diseases in citrus leaves. The use of ATR-FTIR enables measurements with leaves without any sample preparation, which makes the analysis process faster (by a few minutes). In this study, a method was developed using the combination of ATR-FTIR spectroscopy with an induced classifier via PLSR applied to leaves for diagnosis of diseases in Valencia sweet orange. The total success rate of the method was around 94%. It is important to emphasize that the method differentiated healthy from HLB-asymptomatic leaves with success rate greater than 95%. The high accuracy rate may be related to variations in the concentration of carbohydrates and secondary metabolites, such as hesperidin and umbelliferone. While hesperidin is one of the secondary metabolites of citrus with the highest concentration in the leaves of Valencia sweet orange, umbelliferone is a coumarin involved in plant defense against pathogens and is also a precursor of other coumarins produced for the same purpose. Further analyses should investigate which substances are changing in the evolution of citrus diseases and which ones contribute most to the diagnosis of diseases in citrus trees.

The major advantages of the method developed here are the high accuracy rate and the speed of the analysis process, both of which enable the use of a large-scale diagnostic tool for citrus diseases aimed at the construction of infestation maps, and, thus provide a more efficient means of control.

References

[1] Food and Agriculture Organization of the United Nations, Available at: http://faostat.fao.org/site/567/DesktopDefault.aspx?PageID=567#ancor, Accessed: 9/9/2011.
[2] M.A.V. Sluys, M.C. de Oliveira, C.B. Monteiro-Vitorello, C.Y. Miyaki, L.R. Furlan, L.E.A. Camargo, A.C.R. da Silva, D.H. Moon, M.A. Takita, E.G.M. Lemos, M.A. Machado, M.I.T. Ferro, F.R. da Silva, M.H.S. Goldman, G.H. Goldman, M.V.F. Lemos, H. El-Dorry, S.M. Tsai, H. Carrer, D.M. Carraro, R.C. de Oliveira, L.R. Nunes, W.J. Siqueira, L.L. Coutinho, E.T. Kimura, E.S. Ferro, R. Harakava, E.E. Kuramae, C.L. Marino, E. Giglioti, J. Bacteriol. 185 (2003) 1018–1026.
[3] J.M. Bové, A.J. Ayres, IUBMB Life 59 (2007) 346–354.
[4] A. Souza, M. Takita, H. Coletta-Filho, C. Caldana, G. Goldman, N. Muto, R. de Oliveira, L. Nunes, M.A. Machado, Mol. Plant Microbe Interact. 16 (2003) 867–875.
[5] J.M. Bové, J. Plant Pathol. 88 (2006) 7–37.
[6] J. Belasque Junior, A. Bergamin Filho, R.B. Bassanezi, J.C. Barbosa, N.G. Fernandes, P.T. Yamamoto, S.A. Lopes, M.A. Machado, R.P. Leite Junior, A.J. Ayres, C.A. Massari, Trop. Plant Pathol. 34 (2009) 137–145.
[7] T.R. Gottwald, J.V. Graça, R.B. Bassanezi, Plant Health Prog. (2007) (Online, doi:10.1094/PHP-2007-0906-01-RV).
[8] T.M. Spann, R.A. Atwood, M.M. Dewdney, R.C. Ebel, R. Ehsani, G. England, S. Futch, T. Gaver, T. Hurner, C. Oswalt, M.E. Rogers, F.M. Roka, M.A. Ritenour, M. Zekri, Citrus Ind. 91 (2010) 6–13.
[9] J. Fan, C. Chen, R.H. Brlansky, F.G. Gmitter Jr., Z.G. Li, Plant Pathol. 59 (2010) 1037–1043.
[10] D.S. Achor, E. Etxeberria, N. Wang, S.Y. Folimonova, K.R. Chung, L.G. Albrigo, Plant Pathol. J. 9 (2010) 56–64.
[11] E. Etxeberria, P. Gonzalez, D. Achor, G. Albrigo, Physiol. Mol. Plant Phytol. 74 (2009) 76–83.
[12] S. Sankaran, R. Ehsani, E. Etxeberria, Talanta 83 (2010) 574–581.
[13] A.B. Ribeiro, P.V. Abdelnur, C.F. Garcia, A. Belini, V.G.P. Severino, M.F.G.F. Da Silva, J.B. Fernandes, P.C. Vieira, S.A. de Carvalho, A.A. de Souza, M.A. Machado, J. Agric. Food Chem. 56 (2008) 7815–7822.
[14] R. Hammerschmidt, Annu. Rev. Phytopathol. 37 (1999) 285–306.
[15] U. Afek, A. Sztejnberg, Phytopathology 79 (1989) 736–739.
[16] U. Afek, J. Orenstein, S. Carmeli, V. Rodov, M. Joseph, Phytochemistry 50 (1999) 1129–1132.
[17] D.C. Teixeira, C. Saillard, C. Couture, E.C. Martins, N.A. Wulff, S. Eveillard-Jagoueix, P.T. Yamamoto, A.J. Ayres, J.M. Bové, Mol. Cell. Probes 22 (2008) 139–150.
[18] W. Li, J.S. Hartung, L. Levy, J. Microbiol. Methods 66 (2006) 104–115.
[19] X. Qin, V.S. Miranda, M.A. Machado, E.G.M. Lemos, J.S. Hartung, Phytopathology 91 (2001) 599–605.

[20] L.A. Peroni, J.R.R. dos Reis, H.D. Coletta-Filho, A.A. de Souza, M.A. Machado, D.R. Stach-Machado, J. Microbiol. Methods 75 (2008) 302–307.

[21] F.M.V. Pereira, D.M.B.P. Milori, A.L. Venâncio, M.S.T. Russo, P.K. Martins, J. Freitas-Astúa, J. Anal. At. Spectrom. 25 (2010) 351–355.

[22] F.M.V. Pereira, D.M.B.P. Milori, A.L. Venâncio, M.S.T. Russo, P.K. Martins, J. Freitas-Astúa, Talanta 83 (2010) 351–356.

[23] F.M.V. Pereira, D.M.B.P. Milori, E.R. Pereira Filho, A.L. Venâncio, M.S.T. Russo, P.K. Martins, J. Freitas-Astúa, Anal. Methods 3 (2011) 552–556.

[24] F.M.V. Pereira, D.M.B.P. Milori, E.R. Pereira Filho, A.L. Venâncio, M.S.T. Russo, M.C.B. Cardinali, P.K. Martins, J. Freitas-Astúa, Comput. Electron. Agric. 79 (2011) 90–93.

[25] S.A. Hawkins, B. Park, G.H. Poole, T.R. Gottwald, W.R. Windham, J. Albano, K.C. Lawrence, J. Agric. Food Chem. 58 (2010) 6007–6010.

[26] S.A. Hawkins, B. Park, G.H. Poole, T.R. Gottwald, W.R. Windham, K.C. Lawrence, Appl. Spectrosc. 64 (2010) 100–103.

[27] S. Wold, M. Sjöström, L. Eriksson, Chemom. Intell. Lab. Syst. 58 (2001) 109–130.

[28] E. Frank, Y. Wang, S. Inglis, G. Holmes, I.H. Witten, Mach. Learn. 32 (1998) 63–76.

[29] Spectral Database for Organic Compounds, National Institute of Advanced Industrial Science and Technology (AIST), 2011, Available at: http://riodb01.ibase.aist.go.jp/sdbs/cgi-bin/direct_frame_top.cgi, Accessed: 10/30/2011.

[30] S. Kawaii, Y. Tomono, E. Katase, K. Ogawa, M. Yano, M. Koizumi, C. Ito, H. Furukawa, J. Agric. Food Chem. 48 (2000) 3865–3871.

[31] M.A. Hall, E. Frank, G. Holmes, B. Pfahringer, P. Reutemann, I.H. Witten, SIGKDD Explor. 11 (2009) 10–18.